Translational Oncology

www.transonc.com

Volume 2 Number 4 December 2009 pp. 341–349

Expression Profiling of the Ovarian Surface Kinome Reveals Candidate Genes for Early Neoplastic Changes[1,2]

Tanja Pejovic*, Nupur T. Pande*, Motomi Mori†, Paulette Mhawech-Fauceglia‡, Christina Harrington†, Solange Mongoue-Tchokote†, Daniel Dim‡, Christopher Andrews§, Amy Beck¶, Yukie Tarumi*, Jovana Djilas*, Fabio Cappuccini*, Otavia Caballero#, Jiaqi Huang, Samuel Levy**, Alexia Tsiamouri**, Joanna Cain*, Grover C. Bagby††, Robert L. Strausberg**, Andrew J. Simpson# and Kunle O. Odunsi¶,‡‡**

*Division of Gynecologic Oncology, Oregon Health & Science University, Portland, OR 97239, USA; †Knight Cancer Institute, Portland, OR 97239, USA; ‡Division of Pathology, Roswell Park Cancer Institute, Buffalo, NY 14263, USA; §Division of Biostatistics, Roswell Park Cancer Institute, Buffalo, NY 14263, USA; ¶Division of Gynecologic Oncology, Roswell Park Cancer Institute, Buffalo, NY 14263, USA; #Ludwig Institute for Cancer Research, New York Branch at Memorial Sloan-Kettering Cancer Center, New York, NY 10021, USA; **J. Craig Venter Institute, Rockville, MD, USA; ††Division of Hematology and Oncology, Oregon Health & Science University, Portland, OR 97239, USA; ‡‡Division of Immunology, Roswell Park Cancer Institute, Buffalo, NY 14263, USA

Abstract

OBJECTIVES: We tested the hypothesis that co-coordinated up-regulation or down-regulation of several ovarian cell surface kinases may provide clues for better understanding of the disease and help in rational design of therapeutic targets. *STUDY DESIGN:* We compared the expression signature of 69 surface kinases in normal ovarian surface epithelial cells (OSE), with OSE from patients at high risk and with ovarian cancer. *RESULTS:* Seven surface kinases, *ALK*, *EPHA5*, *EPHB1*, *ERBB4*, *INSRR*, *PTK*, and *TGFβR1* displayed a distinctive linear trend in expression from normal, high-risk, and malignant epithelium. We confirmed these results using semiquantitative reverse transcription–polymerase chain reaction and tissue array of 202 ovarian cancer samples. A strong correlate was shown between disease-free survival and the expression of *ERBB4*. DNA sequencing revealed two novel mutations in *ERBB4* in two cancer samples. *CONCLUSIONS:* A distinct subset of the ovarian surface kinome is altered in the transition from high risk to invasive cancer and genetic mutation is not a dominant mechanism for these modifications. These results have significant implications for early detection and targeted therapeutic approaches for women at high risk of developing ovarian cancer.

Translational Oncology (2009) 2, 341–349

Address all correspondence to: Dr. Tanja Pejovic, Gynecologic Oncology, Oregon Health & Science University, L466, 3181 SW Sam Jackson Park Rd, Portland, OR 97239. E-mail: pejovict@ohsu.edu or Dr. Kunle Odunsi, Gynecologic Oncology, Roswell Park Cancer Institute, Elm & Carlton Streets, Buffalo, NY 14263.

[1]The study was supported by the Cancer Research Institute's Ovarian Cancer Working Group Grant (K.O. and A.J.S.) and the Hilton-Ludwig Cancer Metastasis Grant of the Ludwig Institute for Cancer Research (K.O. and T.P.), grant support from the Department of Veterans Affairs and National Institutes of Health (HL72321 and HL048546) (G.C.B.), the Reproductive Malignancies Program of the Oregon Health & Science University Cancer Institute, Mr. and Mrs. Richard A. Rubinstein, the Sherrie Hildreth Ovarian Cancer Foundation, and the Columbia River Yacht Club.

[2]This article refers to supplementary materials, which are designated by Tables W1 to W3 and are available online at www.transonc.com.

Received 28 July 2009; Revised 24 August 2009; Accepted 28 August 2009

 1944-7124

DOI 10.1593/tlo.09199

Introduction

Approximately 2% of human genome, corresponding to 433 to 518 genes, code for kinases, which are collectively referred to as the kinome. The human kinome is involved in multiple functions in the life cycle of cells, and their differential expression in cancer suggests that protein kinases play an important role in tumor progression and proliferation. The pivotal role of individual kinases in the aggressive clinical behavior of epithelial ovarian cancer (EOC) has been previously demonstrated in studies of v-erb-b2 erythroblastic leukemia viral oncogene homolog-2 (*ERBB-2*), vascular endothelial growth factor (*VEGF*), and v-erb-b2 erythroblastic leukemia viral oncogene homolog-3 (*ERBB-3*) [1–3]. Here, we propose that analysis of co-coordinated up-regulation or down-regulation of several kinases not only will provide more useful understanding of the disease but also could help in the rational design of therapeutic targets in EOC.

Differential gene expression profiling with microarray technology provides a powerful tool to detect and delineate specific signaling pathways that may be dysregulated in cancer. In the current study, we evaluated the expression pattern of the human kinome in EOC. We analyzed kinome expression in ovarian surface epithelial cells (OSE) obtained from patients with normal, high-risk, and cancerous ovaries using Affymetrix expression array HG-U133 Plus2. We combined *in silico* data mining with a detailed literature review to identify a group of 69 genes encoding for cell surface kinases, which may be targets for small molecule inhibitors and antibodies. Our analysis led to the identification of 10 surface kinases differentially expressed in cancer compared with normal ovarian tissue. Although the kinome profile of OSE from "high-risk" ovaries did not seem to be different from normal ovaries, there was a clear linear trend in 7 of the 10 genes with increased/decreased expression from normal to high risk to cancer tissues. These were anaplastic lymphoma kinase (*ALK*), Eph receptor A5 (*EPHA5*), Eph receptor B1 (*EPHB1*), v-erb-b2 erythroblastic leukemia viral oncogene homolog-4 (*ERBB4*), insulin receptor-related receptor (*INSRR*), protein tyrosine kinase 7 (*PTK7*), and transforming growth factor, β receptor 1 (*TGFβR1*). Finally, we validated these observations by tissue microarray (TMA) analysis for four of the seven genes as well as by reverse transcription–polymerase chain reaction (RT-PCR). Together, our study demonstrates that differential expression of kinases could represent early changes in EOC, priming it for transformation and a multimodal strategy targeting these kinases could represent a novel therapeutic strategy.

Materials and Methods

Specimen Collection

A total of 18 ovarian samples were collected under an approved institutional review board protocol (Oregon Health & Science University, IRB #921). The samples were obtained fresh in the operating room from women undergoing surgery for benign gynecologic disease, from patients with stage IIIC poorly differentiated ovarian carcinoma at the time of initial tumor staging/debulking procedure, and from women undergoing risk-reducing oophorectomy because of significantly elevated risk of developing ovarian cancer. The patients were considered to be at high risk for ovarian cancer if they had two or more first-degree relatives with ovarian and/or breast cancer or they had a personal history of breast cancer and a first-degree relative with breast and/or ovarian cancer. For this study, we selected high-risk patients that were negative for *BRCA1* and *BRCA2* mutations. The numbers of samples and subjects for each group were as follows: five cancer samples (5 subjects), six normal samples (4 subjects), and seven high-risk samples (5 subjects).

OSE Preparation

Ovarian tissue was mechanically minced in 5 ml of Dulbeccos phosphate-buffered saline at room temperature and digested with 5 ml of 0.2% trypsin (Sigma-Aldrich, St Louis, MO) overnight at 4°C. Dissociated epithelial cells were cultured in collagen-coated 35-mm Petri dish in sterile OSE culture medium (1:1 mixture of RPMI-1640 and Dulbecco's modified Eagle's medium, 20% FBS, 10 μg/ml insulin, 10 ng/ml epidermal growth factor, 1% Pen/Strep, and 0.1% gentamicin) in a 5% CO_2 incubator at 37°C for at least 96 hours. When confluent, the cells were trypsinized (5 mg/ml Trypsin +7 mM EDTA; Sigma-Aldrich) and subcultured or harvested for RNA or protein.

Antibodies

Four commercially available primary antibodies were used including the polyclonal antibodies to ERBB4, EPHA5, and TGFβR1 (Abgent Envision Proteomics, San Diego, CA) and a monoclonal antibody to INSRR (R&D Systems, Minneapolis, MN). The control antibodies to calnexin and α-tubulin were obtained from Sigma-Aldrich. Detection was performed using the avidin-biotin-peroxidase complex method (LASB Kit; Dakocytomation, Glostrup, Denmark).

RNA Isolation and Sample Preparation

Approximately 3×10^6 OSE cells were used for the extraction of total RNA by homogenization in a guanidinium isothiocyanate–based buffer (RNeasy Micro Kit; Qiagen, Valencia, CA) according to manufacturer's instructions. The integrity of the RNA was evaluated by a Bioanalyzer (Agilent, Palo Alto, CA). The RNA specimens were analyzed using Affymetrix oligonucleotide array, HG-U133 Plus 2.0 (Affymetrix, Santa Clara, CA), which contains more than 54,675 probe sets representing 47,000 transcripts and variants as well as 38,500 well-characterized human genes. Each RNA sample was labeled using a two-step labeling process. In the first step, messenger RNA (mRNA) was converted to double-stranded complementary DNA (cDNA) using Reverse Transcriptase (Invitrogen, Carlsbad, CA) and an oligo-dT primer linked to a T7 RNA polymerase binding site sequence (IDT, Coralville, IA). *In vitro* transcription was performed in the second step where the cDNA was converted to labeled complementary RNA (the target) using T7 RNA polymerase in the presence of biotinylated UTP and CTP (Enzo Life Science, Farmingdale, NY). After this linear amplification, the target was chemically fragmented to produce a uniform distribution of short complementary RNA (cRNA). Fragmented, biotinylated targets (cRNA fragments) were combined with hybridization control oligomer (Affymetrix) and control cRNA (1.5 pM BioB, 5.0 pM BioC, 25 pM BioD, and 100 pM Cre-cRNA) in hybridization buffer and applied to the HG-U133 Plus 2.0 array, which was packaged in a self-contained cartridge. The overnight hybridization was followed with staining using streptavidin-phycoerythrin (SAPE; Molecular Probes, Eugene, OR). Signal amplification was performed using a biotinylated antistreptavidin antibody (Vector Labs, Burlingame, CA), followed by a second staining with SAPE. Scans of the processed chip were performed using the GeneArray Laser Scanner (Affymetrix).

Gene Expression Analysis

The GeneChip Operating Software (GCOS) was used for image analysis and signal quantification. The sample performance was evaluated using QC/QA parameters including: background, noise (*Q*),

average signal intensity, and ratio of signal intensities for probe sets representing the 5′ and 3′ ends of actin and GAPDH transcripts. Targets that do not meet predetermined thresholds were remade whenever possible or discarded from further analysis. In addition, each array was visually inspected for scratches and nonuniform intensity patterns that may affect chip performance. After the initial inspection, one cancer sample was excluded from the statistical analysis owing to poor RNA quality. Signal data from 17 remaining samples (4 cancers, 6 normal, and 7 high risks) were normalized using Robust Multiarray Average using R Bioconductor (http://www.bioconductor.org/). After normalization, the data were examined visually using the box-plot of each sample, hierarchical clustering of samples, and multidimensional scaling of samples based on all 54,675 probe sets. After verifying the data quality, we selected 203 probe_sets that represented 69 preselected kinase genes.

EST and SAGE (Serial Analysis of Gene Expression) data set generated in our laboratory, combined with all other publicly available human transcript data, the Oncomine Microarray Database (http://141.214.6.50/oncomine/main/index.jsp) was used to identify 69 members of the Ovarian Surface Kinome as listed in Table W1. For each of the selected 203 probe sets for these kinases, we performed analysis of variance to compare the mean expression levels among cancer, high-risk, and normal groups. In addition, a linear contrast was generated to determine whether there was a linear trend between normal, high-risk, and cancer samples. Owing to the small sample size, we did not adjust for potential within-subject correlation and treated each sample as an independent observation, although some patients provided more than one sample. The resulting *P* values from *F*-statistics were adjusted for multiple comparisons using the false discovery rate (FDR) of Benjamini and Hochberg [4]. The mean differences between groups were converted to the mean fold change (FC) by taking anti-log (base 2). Specifically, let Δ = mean difference ($\log_2$ scale). Then FC was defined as: $2^{|\Delta|}$, if $\Delta \geq 0$, and $-2^{|\Delta|}$, if $\Delta < 0$. Therefore, FC = 2 implies two-fold change in the positive direction (up-regulation), whereas FC = −2 implies two-fold change in the negative direction (down-regulation). Genes with FDR less than 15% are considered differentially expressed and subsequently analyzed by DNA sequencing and tissue arrays. All statistical analyses were performed using Statistical Analysis System [5]. Affymetrix NetAffx Center (http://www.affymetrix.com/analysis/index.affx) was used to obtain additional biologic information on differentially expressed genes. Annotation information included the putative gene description, as well as external identifiers to UniGene and LocusLink, Gene Ontology (GO) functions, and pathway information [6].

Tissue Microarray Preparation

Paraffin-embedded tissues from 202 patients with ovarian cancer were used to construct the microarrays as described previously by Kononen et al. [7]. Sections were incubated with ERBB4, EPHA5, TGFβR1, and INSRR antibodies at room temperature. The biotin-free HRP enzyme-labeled polymer of the Envision Plus Detection System (Dakocytomation) was used as a secondary reagent. The diaminobenzidine complex was used as a chromogen. In negative controls, a normal goat serum was used instead of the primary antibody. The extent of immunochemical reactivity was graded based on intensity as follows: 0 (negative), 1+ (weak), 2+ (moderate), 3+ (strong). Negative control slides omitting the primary antibody were included in all assays. Every attempt was made to evaluate OSE staining only; however, that was not entirely possible in cancer cases because of the almost complete change of surface architecture.

Semiquantitative Reverse Transcription

One microgram of RNA from two normal, two high-risk, and two cancer samples (from the initial cohort of 18 patients) was reverse-transcribed in the presence of 50-nM random hexamer (NEB, Ipswich, MA) and AMV Reverse Transcriptase (Promega, Madison, WI) by incubating at 65°C for 5 minutes followed by cooling on ice for 5 minutes and then synthesizing the cDNA at 48°C for 40 minutes. PCR was subsequently performed to analyze expression of *ALK*, *EPHA5*, *EPHB1*, *ERBB4*, *INSRR*, *PTK7*, and *TGFβR1*. The primers are listed in Table W2.

Amplification for all gene products was for 1 minute at 94°C and for 30 or 35 cycles at 94°C for 30 seconds, 60°C for 30 seconds, and 72°C for 45 seconds. A final extension cycle at 72°C for 10 minutes was designed at the end of cycling to ensure complete synthesis. The PCR products were visualized by separation on a 3% agarose gel after staining with ethidium bromide. The assessment of FC was made by scanning the images and subsequent densitometry of the signal using Quantity One 1-D Analysis Software (Bio-Rad Laboratories, Hercules, CA). Relative changes were calculated by determining the ratio of experimental signal intensity to that of the internal control (normalized GAPDH signal) for each sample for each probe set. The fold increase is represented as compared with the signals from normal samples for each normalized gene. The standard deviation representative of variance between three independent replicates was calculated.

DNA Sequencing

Twenty-nine pairs of primary poorly differentiated serous stage IIIC ovarian carcinomas samples with matched normal blood DNA samples were used in mutation screening. Multiple displacement amplification (MDA) was performed to provide sufficient quantities of DNA for mutation screening. One hundred nanograms of genomic DNA from samples was subjected to MDA. The reaction volume was 250 μl with an expected yield of 150 to 250 μg of MDA-DNA as measured by double-stranded DNA quantification (PicoGreen; Invitrogen). Two diagnostic loci (WIAF-1004 and WIAF-699) in the MDA-DNA were analyzed by real-time quantitative PCR for ensuring the integrity of the amplified sample. A locus representation of 100% indicates nonbiased amplification of the original genomic DNA. The analysis revealed that all samples correspond to the "highly usable" category defined by greater than 3% of locus representation with a ratio of less than 20-fold between the two loci. The genetic identities of 29 matching normal and ovarian cancer DNA (GBM19) were confirmed by 16 highly polymorphic markers. Seven receptor kinase genes showing linear trend in expression from normal to high risk to cancer (*ALK*, *EPHB1*, *EPHA5*, *ERBB4*, *TGFβR1*, *INSRR*, and *PTK7*) were selected for mutation screening. Coding exons and intron-exon splicing junctions of selected genes were sequenced. Detailed methods for primer design, PCR sequencing, and data analysis are described elsewhere [8]. All primer sequences are available on request.

TMA Statistical Analysis

An independent set of 202 ovarian cancer samples arranged as TMA was analyzed for statistical correlates, as described in the section for gene expression. Clinical variables were available for all 202 cases and are summarized with proportions, means, or quartiles as described in the Results section. Kendall τ was used to measure the association between

Table 1. Human Kinome Genes Upregulated or Downregulated among Normal (N), High-Risk (HR), and Cancer (C) Samples ($P < .15$).

Probe Set ID	Gene* Symbol	HR *vs* N, Adjusted *P*	HR *vs* N, FC	HR *vs* N, Change	C *vs* HR, Adjusted *P*	C *vs* HR, FC	C *vs* HR, Change	C *vs* N, Adjusted *P*	C *vs* N, FC	C *vs* N, Change
208212_s_at	*ALK*	0.214	1.2141	No Change	0.7029	1.07	No Change	0.0572	1.2991	Up
202686_s_at	*AXL*	0.5475	−1.1746	No Change	0.0864	1.5104	Up	0.4068	1.2859	No Change
203499_at	*EPHA2*	0.2737	−1.5464	No Change	0.052	1.8854	Up	0.5547	1.2192	No Change
215664_s_at	*EPHA5*	0.8856	1.0971	No Change	0.052	2.6911	Up	0.0561	2.9525	Up
237939_at	*EPHA5*	0.9119	1.0421	No Change	0.037	2.6485	Up	0.0331	2.7601	Up
241404_at	*EPHA5*(1)	0.8932	1.0617	No Change	0.052	2.3999	Up	0.0561	2.5479	Up
210753_s_at	*EPHB1*	0.9119	1.0265	No Change	0.052	1.6876	Up	0.0561	1.7324	Up
211898_s_at	*EPHB1*	0.9119	−1.0179	No Change	0.052	1.3723	Up	0.0776	1.3482	Up
217324_at	*EPHB1*(2)	0.2737	1.167	No Change	0.8363	1.0405	No Change	0.0776	1.2143	Up
230425_at	*EPHB1*	0.7541	−1.3002	No Change	0.068	4.7333	Up	0.1857	3.6403	No Change
241581_at	*ERBB4*(3)	0.4725	1.102	No Change	0.3951	1.1199	No Change	0.0776	1.2341	Up
215776_at	*INSRR*	0.2737	1.1672	No Change	0.8969	1.0236	No Change	0.1462	1.1948	Up
203131_at	*PDGFRA*	0.5261	1.4736	No Change	0.052	−3.084	Down	0.2339	−2.0928	No Change
1555324_at	*PTK7*	0.3554	−1.3193	No Change	0.6761	−1.1565	No Change	0.0776	−1.5257	Down
224793_s_at	*TGFBR1*	0.7272	1.132	No Change	0.1564	1.6893	No Change	0.0776	1.9122	Up
236561_at	*TGFBR1*	0.9442	1.0141	No Change	0.052	1.6841	Up	0.0671	1.7078	Up

(1), *(2)*, and *(3)* indicates that the gene symbol was unavailable in March 2008 annotation. The other 13 annotations are unchanged.
*Gene symbols are based on June 2005 Annotations from the Netaffx Analysis Center (http://www.affymetrix.com/analysis/index.affx).

ordered variables such as the staining intensities of EPHA5, ERBB4, INSRR, and TGFβR1. Kaplan-Meier method was used to estimate disease-free survival (DFS) as well as overall survival (OS), and log-rank tests were used to compare survival curves between groups defined by the staining intensity for each gene. Confidence intervals for survival curves were based on asymptotic Wald statistics on log scale.

Results

The Expression Profile of Ovarian Surface Kinome

The examination of selected 69 cell surface kinase expression represented by a total of 203 probe_set IDs in OSEs revealed a total of 10 genes (16 probe_sets) that were differentially expressed in at least one of the three paired comparisons between normal, high-risk, and cancer groups. Of these, 7 genes (12 probe_sets) were differentially expressed (i.e., FDR adjusted, $P < .15$) between cancer and normal groups (Table 1). Six genes (10 probe_sets) were differentially expressed between cancer and high-risk OSEs. The overlap between these two subsets involved three genes: *EPHA5*, *EPHB1*, and *TGFβR1*. None of the total 203 probe sets were differentially expressed between normal *versus* high-risk OSEs.

We performed a linear trend analysis for all 10 genes. Seven genes, *ALK*, *EPHA5*, *EPHB1*, *ERBB4*, *INSRR*, *PTK7*, and *TGFβR1*, displayed a distinctive linear trend of expression from normal to high risk to cancer (Figure 1). The seven genes showing a linear trend of expression are the same seven genes found to be differentially expressed in comparison between cancer and normal groups.

DNA Sequencing Revealed Two Independent Intronic Mutations in ERBB4

To test whether observed alterations in gene expression are a consequence of genetic mutations, bidirectional dideoxy sequencing using the high-throughput sequencing pipeline at the Venter Institute's Joint

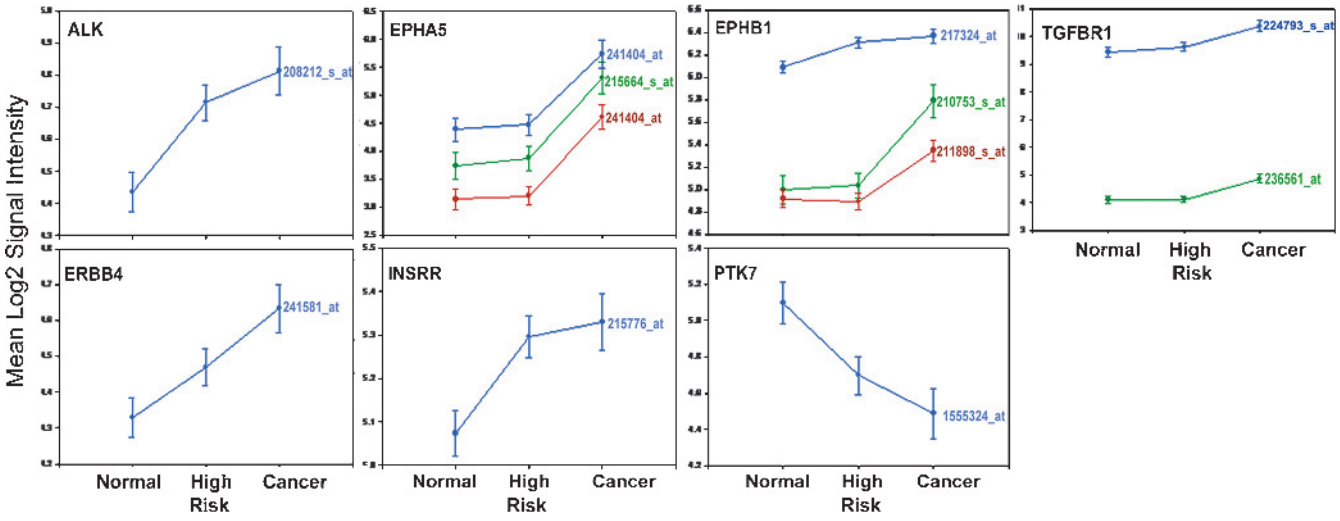

Figure 1. Linear trend of expression for the seven differentially expressed genes. The normalized mean Log2 intensities with 95% confidence interval were plotted on the *y*-axis and the probeset_ids for each ordinal group on the *x*-axis. Different color lines denote each probe_set across the three experimental groups. *ALK*, *EPHA5*, *EPHB1*, *ERBB4*, and *INSRR* show an increasing trend, whereas *PTK7* seems to be negatively modulated.

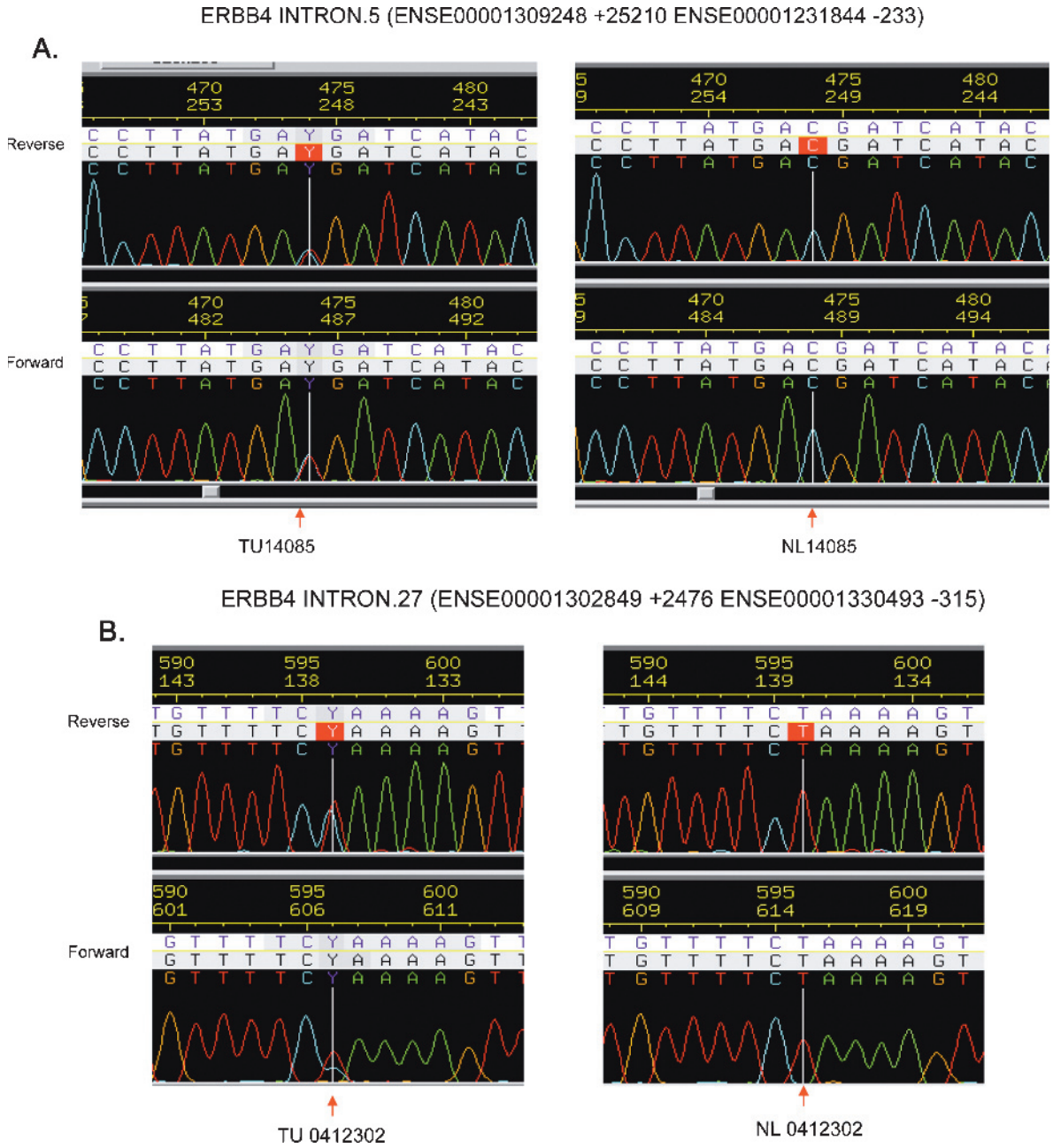

Figure 2. Somatic point mutations in *ERBB4* gene in two ovarian carcinomas by resequencing. The panels on the left show forward and reverse sequence trace file from tumor and the right panel shows matched blood sample. (A) Intron 5 displayed a mutation in matched samples from tissue and blood. An acquired T/T to T/C mutation is identified in intron 5 as highlighted base in the trace. (B) Intron 27 C/C to C/T acquired mutation is identified in the sequence panel as a highlighted base. For full description, see Results section.

Technology Center was performed. Two novel mutations were detected in *ERBB4* in two different cancer samples. A somatic mutation C/C to C/T was identified in intron 5 in the cancer sample TU14085 (Figure 2*A*). The mutation was located at 25,210-bp 3′ of exon 5 (ENSE00001309248) and 233-bp 5′ of exon 6 (ENSE00001231844). A somatic mutation T/T to T/C was identified in intron 27 in tumor TU0412302 (Figure 2*B*). The mutation was located at 2476-bp 3′ of exon 27 (ENSE00001302849) and 315-bp 5′ of exon 28 (ENSE00001330493). Representative sequence traces are shown in Figure 2 (*A* and *B*). The functional consequences of the two mutations are uncharacterized; however, the association of intron 5 mutation with ErbB4 protein overexpression in TU14085 (data not shown) may suggest a functional significance of the mutation. We found no mutations in *ALK*, *EPHA5*, *EPHB1*, *INSRR*, *TGFβR1*, and *PTK7*.

Select Kinases Are Overexpressed in Most Human Ovarian Cancers

On the basis of the results of our gene expression studies, DNA sequencing studies, and availability of antibodies, we selected a subset of genes (*EPHA5*, *ERBB4*, *INSRR*, and *TGFβR1*) for further validation at the protein level. Immunohistochemistry was used to test an independent set of 202 ovarian cancer samples of all stages in TMA. Scored staining profile is shown in Table 2*A*. The ERBB4 staining was positive in 195, EPHA5 in 177, TGFβR1 in 105, and INSRR in 97 of the 202.

Table 2. TMA Profile of Ovarian Carcinoma.

(A) Immunocytochemistry: Intensity and Pattern of Staining for the Four Chosen Antibodies

Intensity	TGFβR1		ErbB-4		EphA5		INSRR	
	No. Cases/Total	Percentage, %	No. Cases/Total	Percentage, %	No. Cases/Total	Percentage, %	No. Cases/Total	Percentage, %
0	94	46.5	2	1.0	16	7.9	2	1.0
1	58	28.7	39	19.3	66	32.7	11	5.4
2	24	11.9	44	21.8	60	29.7	43	21.3
3	23	11.4	112	55.4	51	25.2	43	21.3
3 N/A	0	0.0	5	2.5	9	4.5	0	0.0
Pattern of staining in the TMA being studied								
Nuclear	77	38.1	75	37.1	2	1.0	0	0.0
Nonnuclear	118	58.4	120	59.4	118	58.4	99	49.0

(B) Semiquantitative RT-PCR: Relative Intensity of Select Kinases in Normal, High-Risk, and Cancer Cells

Gene	Sample Type	Normalized Mean FC with Respect to Normal*,†	SD
ERBB4	Normal	1.00	0.089
	High risk	2.64	0.023
	Cancer	5.24	0.115
EPHB1	Normal	1.00	0.193
	High risk	1.99	0.038
	Cancer	10.69	0.441
PTK7	Normal	1.00	0.170
	High risk	0.45	0.152
	Cancer	0.19	0.070
TGFβR1	Normal	1.00	0.243
	High risk	1.85	0.109
	Cancer	2.92	0.102

*The signal intensities expressed in arbitrary units were adjusted for the background intensities for that lane and then the resulting intensities from three experiments were averaged.
†Normalized ratios were calculated by dividing the normalized intensities by the values obtained for normal tissue for that gene.

The pattern of staining differed among the markers: ERBB4 demonstrated intense cytoplasmic, nuclear, and membranous staining. In contrast, EPHA5 reactivity was predominantly cytoplasmic and, to a lesser degree, nuclear (Table 2*A*), and INSRR resulted in exclusively cytoplasmic staining. The TGFβR1 staining pattern appeared to be diffuse cytoplasmic, whereas INSRR staining appeared to be in punctate bodies around the nucleus or cell junctions (Table 2*A*).

Several associations were observed. The intensity of staining for ERBB4 and EPHA5 was positively correlated ($\tau = 0.38$, $P < .0001$) as well as that for ERBB4 and TGFβR1 ($\tau = 0.13$, $P < .049$) and for EPHA5 and TGFβR1 ($\tau = 0.12$, $P < .048$). The nuclear staining pattern was associated with a higher staining intensity for both ERBB4 and EPHA5 ($P < .0001$ each).

Several disease associations were observed. The intensity of staining for ERBB4 and EPHA5 was positively correlated ($\tau = 0.38$, $P < .0001$) as well as that for ERBB4 and TGFβR1 ($\tau = 0.13$, $P < .049$) and for EPHA5 and TGFβR1 ($\tau = 0.12$, $P < .048$). The nuclear staining pattern was associated with higher staining intensity for both ERBB4 and EPHA5 ($P < .0001$ each).

TMA and Clinical Correlation

The characteristics of study population are presented in Table 3. The median age was 61 years (range, 33-89 years). Most patients presented with grade 3 tumors (84%), stage IIIC (77%), and with serous histologic diagnosis (77%). A complete response to therapy was achieved in 98 (49%) of the 202, a partial response was achieved in 97 (48%) of the 202, whereas the remaining 7 patients showed no response. The median estimated OS for all patients was 40.8 months (confidence interval [CI], 30.1-48.0 months), whereas the median DFS was 20.6 months (CI, 17.4-35.9 months). The 5-year DFS and OS for all

Table 3. TMA: Cases Characteristics ($N = 202$).

Age, median (range), years	61 (33-89)
Follow-up (median), months	
FIGO stage, *n* (%)*	
I	8 (4%)
II	10 (5%)
III	155 (77%)
IV	23 (11%)
Histology, *n* (%)*	
Serous	156 (77%)
Clear cell	10 (5%)
Endometrioid	8 (4%)
Mucinous	5 (2%)
Undifferentiated	3 (1%)
Mixed	12 (6%)
Grade, *n* (%)*	
1	9 (4%)
2	16 (8%)
3	169 (84%)
Residual tumor*	
None	64 (32%)
Present	131 (65%)
Clinical response*	
Complete response	98 (49%)
Partial response	97 (48%)
Current status, *n* (%)	
Alive, NED	35 (17%)
Alive with disease	27 (13%)
Dead of disease	134 (66%)
Dead from other causes	6 (3%)

FIGO indicates the International Federation of Gynecology and Obstetrics; *NED*, no evidence of disease.
*Six patients were unstaged (3%), the grade was not determined in 8 (4%), 4 (2%) had carcinosarcoma histologic type, residual tumor and clinical response were not assessed in 7 (3%).

patients in this group were 30.4% (CI, 23.9%-38.6%) and 22.5% (CI, 14.8%-34.3%), respectively. Kaplan-Meier statistics revealed a trend for patients with ERBB4-positive tumors to have a longer DFS and OS, although the association did not reach statistical significance. Log-rank test comparison identified that the gradual increase in both DFS and OS positively correlated with the intensity of ERBB4 staining: patients whose tumors expressed higher ERBB4 staining had a longer DFS ($\chi^2 = 5.0$, $P = .08$; Figure 3, *A* and *B*). Similarly, there was weak evidence that the OS probability is different for different levels of ERBB4 intensity ($\chi^2 = 3.2$, $P = .20$) where higher levels were associated with longer survival (Figure 3*B*). There was no correlation between the pattern of ERBB4 staining (nuclear *vs* membranous) and survival.

Semiquantitative RT-PCR Confirms That a Linear Trend Exists in the Select Group of Surface Kinases between Normal, High-Risk, and Cancer OSE

Semiquantitative PCR was used in an independent set of normal, high-risk, and cancerous primary OSE that were of low passage as a confirmatory assay for changes in *ALK*, *EPHA2*, *EPHA5*, *EPHB1*, *ERBB4*, *INSRR*, *TGFβR1*, and *PTK7*. We found that both methods (microarray analysis and semiquantitative RT-PCR) detected similar patterns for the overexpressed and underexpressed genes selected for validation. The data revealed that in comparison to normal ovarian surface epithelial cells, high-risk OSE demonstrated 2-fold up-regulation of *EPHB1*, 2.6-fold up-regulation of *ERBB4*, 1.8-fold up-regulation of *TGFβR1*, and 0.45-fold down-regulation of *PTK7*. Similar analysis with cancer EOC showed 10.69-fold up-regulation of *EPHB1*, 5.2-fold up-regulation of *ERBB4*, 2.9-fold up-regulation of *TGFβR1*, and approximately 0.2-fold down-regulation of *PTK7*. The quantitative data are shown in Table 2*B*.

Discussion

Protein kinases play a prominent role in many developmental and cellular processes. To identify new oncogenic activation mechanism in ovarian cancer, we studied the surface kinome of OSE derived from individuals who are known to be at significant risk of ovarian cancer based on family history and compared with OSE derived from individuals at low risk and with OSE derived from invasive ovarian cancer. Because *BRCA1/2* mutations account for only a fraction of inherited predisposition to ovarian cancer, mutation carriers were excluded from this analysis in an effort to identify novel oncogenic processes. This study represents the first systematic analysis of the ovarian surface kinome spanning the spectrum of normal, high-risk, and malignant epithelium.

Complementary techniques that included gene expression analysis, semiquantitative RT-PCR, DNA sequence analysis of selected kinases, and independent TMA of ovarian cancer specimens were used as validation in our study. Several novel observations resulted from these sets of experiments. It was anticipated that the magnitude of changes in gene expression between the high-risk and the normal tissue would be subtle at best because the ovaries removed prophylactically from high-risk women are often morphologically and histologically similar to normal ovarian tissues. Indeed, we found no distinction in the expression of the 69 surface receptor kinases between high-risk and normal samples and identified a distinct difference in the expression of a subset of kinases between cancer and high risk on one hand, and cancer and normal ovaries on the other. Significant differences in expression of *EPHA5*, *EPHB1*, and *TGFRβR1* were observed when cancer samples were compared to both normal OSE and high-risk OSE, whereas *AXL*, *EPHA2*, and *PDGFRA* demonstrated a differential expression pattern unique to high-risk OSE. In addition, *ALK*, *INSRR*, *PTK7*,

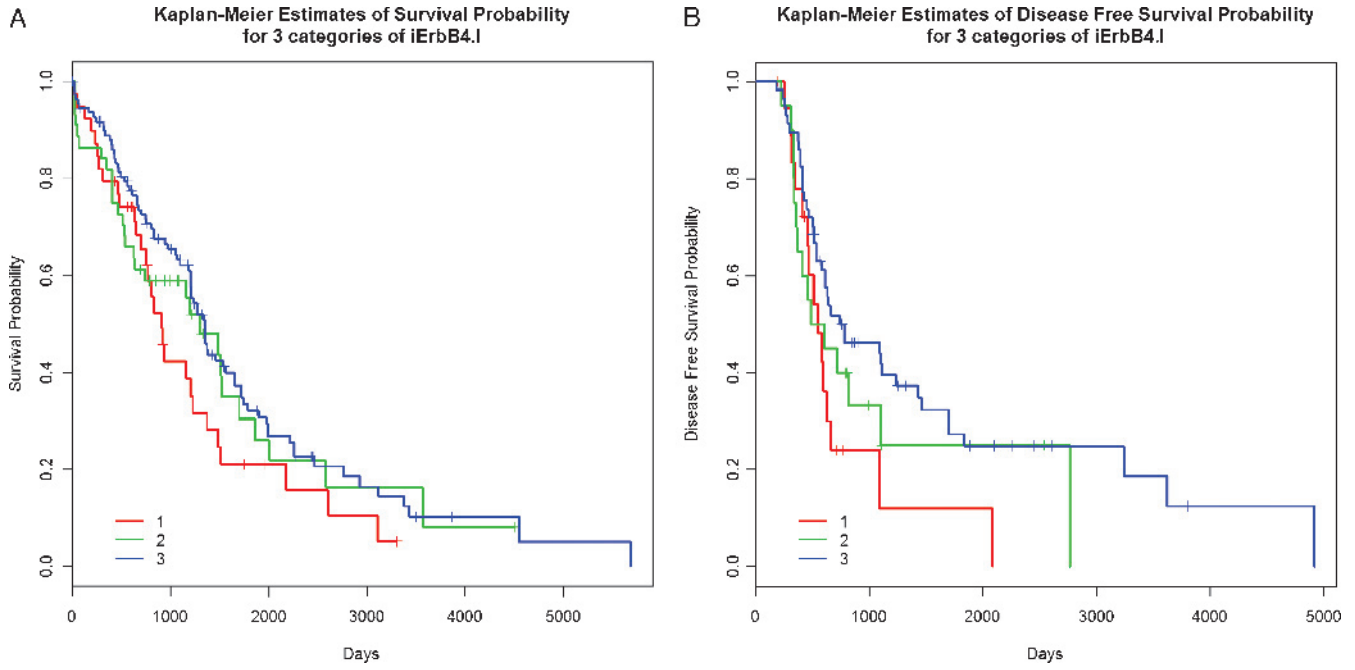

Figure 3. Kaplan-Meier plots showing estimated survival for patients with low, medium or high ERBB4 expression levels. (A) A trend toward longer DFS is associated with a higher ERBB4 expression in ovarian TMA ($P = .08$). The red line represents patients with low ERBB4 expression, green line represents the projected survival for medium levels of ERBB4 protein in the tumors, and the blue line represents highest level of ERBB4 expression. Details of how the levels were assigned are described in the Materials and Methods section. (B) The ERBB4: protein expression and OS. Higher levels of ERBB4 protein expression are associated with longer OS ($P = .2$). 1. Red line = low expression; 2. green line = medium; 3. blue line = high ERBB4 expression level.

and *ERBB4* differential expression was detected between cancer and normal subsets alone. The distinct subset of surface kinases overexpressed when high-risk OSEs are compared with cancer (*EPHA2*, *AXL*, and *PDGFRA*) could be considered critical in the transition from high-risk to frank invasive carcinoma. *AXL* expression has been reported in a wide variety of human cancers including ovarian and shown to be involved in cancer progression [9]. In addition, *EPHA2* was recently shown to promote ovarian tumor growth by enhancing cell–extracellular cell matrix adhesion, increasing anchorage-independent growth, and promoting angiogenesis [10]. Whereas the successive linear transformation of the OSE from normal to high-risk to malignant epithelium seems to be supported by our data from this small cohort of samples, alternative pathway may exist in which accumulation of the genetic changes directly transform a normal cell to the malignant one (Table 1, comparison: Cancer *vs* Normal).

An extended analysis rendered 7 genes within the identified 10 kinase gene set with a significant linear trend of overexpression (*ALK*, *EPHA5*, *EPHB1*, *ERBB4*, *INSRR*, and *TGFβR1*) and underexpression (*PTK7*). To assess the apparent clinicopathologic relevance of the seven kinases identified, a comprehensive expression analysis in a large panel of ovarian carcinoma was performed. Our results indicate that ERBB4 and EPHA5 had the highest frequency of expression in 96% and 87% of the cases, respectively. Increased expression of Eph receptor tyrosine kinases and their respective ephrin ligands has been implicated in tumor progression in a number of malignancies including melanoma, cancer of the breast, prostate, stomach, colon, and small cell lung cancer [11]. Herath et al. [12] reported a striking correlation of *EPHA5* mRNA overexpression with poor survival in ovarian cancer. Because this class of genes is involved in cell-cell communication, it is not surprising that the altered expression in malignancies correlates with increased invasiveness, increased metastatic potential, and poor outcome.

Consistent with previous reports [13], both *ERBB4* mRNA and protein were overexpressed in most samples in our study [13], and the staining was mostly membranous and, to a lesser extent, nuclear [14]. Interestingly, ERBB4 expression in the tumors correlated with both DFS and OS of ovarian cancer patients. The intensity of ERBB4 staining was also positively correlated with survival. The overexpression of ERBB4 has been associated with improved survival in breast cancer patients as well [15]. Although this association has not been functionally explained in either breast or ovarian cancer, it has been shown that ERBB4 modulates cell death pathway [16,17]. Its intracellular domain contains a BH3 subdomain that interacts with BAK, crucial for the death induction and dimerization of BAK, resulting in cytochrome *c* release, heralding apoptosis [16]. It is therefore possible that ERBB4 overexpression predisposes cancer cells toward more efficient apoptosis, which may reflect in longer DFS and OS.

Because distinct isoforms of *ERBB4* and other surface kinases identified in our study could be generated at the transcriptional levels, we also tested whether somatic mutations or polymorphisms may underlie the observed differential expression patterns in the seven genes that demonstrated a linear trend. We sequenced these genes in an independent set of 29 stage III serous ovarian carcinomas. Two independent mutations were identified in the noncoding region of *ERBB4* of two samples. *ERBB4* intron 5 mutation was associated with overexpression of the *ERBB4* mRNA and protein, insinuating that abnormal *ERBB4* mRNA splicing resulted in overexpression of the ERBB4 in tissue. Alternatively, a transcriptional enhancing function of this intronic mutation might exist, influencing transcription elongation. In a previous study, Soung et al. [18] detected a total of 12 mutations in the *ERBB4* gene. These were somatic mutations in 3 (1.7%) of 180 gastric carcinomas, 3 (2.9%) of 104 colorectal carcinomas, 5 (2.3%) of 217 non–small cell lung cancers, and 1 (1.1%) of 94 breast carcinomas. Of the 12 *ERBB4* mutations detected in this study, 3 were found in the introns. The mutations that we report in this study have not been previously defined. Although the functional consequences of the mutation are not known, the intron 27 mutation is located in a conserved base of a FOX03/04 binding site, and the intron 5 mutations is in a conserved base of a CREB transcription factor binding site. This might have an implication in transcriptional regulation of this gene. We are currently exploring this possibility.

We queried the Oncomine database (http://www.oncomine.org) [19] for the expression of the seven kinases in thirteen ovarian cancer studies deposited as of February 2008 (Table W3) [2,18–23]. Each study measured a variety of clinical and pathologic aspects of patients with disease (stage, grade, histologic type, DFS), and they represent 687 independent cases of ovarian cancer. Oncomine expression correlations were searched for each gene, and the results were filtered by selecting ovarian tumors. Statistical analysis of differences was performed using ONCOMINE algorithms to account for the multiple comparisons among different studies, similar to a meta-analysis, as previously described [17]. Interestingly, the Oncomine data largely support some of our results. Notably, *ALK*, *TGFβR1*, *EPHA5*, *INSRR*, and *ERBB4* were dysregulated in more advanced disease stages and associated with more aggressive tumors [2,20,21,23–25]. Similar to our results, Lu et al. [2,20,21,23–25] reported that overexpression of ERBB4 was associated with more favorable 5-year survival.

The results of this study have several implications. First, the critical role for a subset of surface kinases in the progression from "high-risk" OSE to cancer is apparent. Second, a subset of differentially overexpressed surface kinases is shared when normal or high-risk OSE is compared with cancer. Third, the overexpression of one of the surface receptor kinases (*ERBB4*) conferred a higher DFS of the cancer patients. These data suggest that surface receptor kinases (*ALK*, *EPHA5*, *EPHB1*, *ERBB4*, *INSRR*, *PTK*, and *TGFβR1*) could play a role in the early stages of ovarian cancer development, and the lack of somatic mutations in most of these kinases suggest the possibility that posttranscriptional modifications or epigenetic regulation are the dominant mechanisms by which these kinases contribute to OSE cancer development. Even in high-risk individuals with known *BRCA1/2* mutations, these kinases may act as "modifiers" of risk and penetrance. Although the ability to determine the appropriate context to functionally assess the coordinate regulation of the identified surface kinases in this study may be tedious and time consuming, our data indicate that these efforts will be worthwhile to determine whether these kinases should be selected with high priority for molecularly targeted prevention and therapeutic studies.

References

[1] Chen WJ, Chen HW, Yu SL, Huang CH, Wang TD, Chen JJ, Chien CT, Chen HY, Yang PC, and Lee YT (2005). Gene expression profiles in hypoxic preconditioning using cDNA microarray analysis: altered expression of an angiogenic factor, carcinoembryonic antigen–related cell adhesion molecule 1. *Shock* **24**, 124–131.

[2] Lu KH, Patterson AP, Wang L, Marquez RT, Atkinson EN, Baggerly KA, Ramoth LR, Rosen DG, Liu J, Hellstrom I, et al. (2004). Selection of potential markers for epithelial ovarian cancer with gene expression arrays and recursive descent partition analysis. *Clin Cancer Res* **10**, 3291–3300.

[3] Scholl S, Beuzeboc P, and Pouillart P (2001). Targeting HER2 in other tumor types. *Ann Oncol* **12** (Suppl 1), S81–S87.

[4] Benjamini Y and Hochberg Y (1995). Controlling the false discovery rate: a practical and powerful approach to multiple testing. *J R Stat Soc Ser B Methodol* **57**, 289–300.

[5] Cary, NC (1999). *SAS/STAT User's Guide, Version 8*. Cary, NC: STAT Publishing Inc.

[6] Ashburner M, Ball CA, Blake JA, Botstein D, Butler H, Cherry JM, Davis AP, Dolinski K, Dwight SS, Eppig JT, et al. (2000). Gene ontology: tool for the unification of biology. The Gene Ontology Consortium. *Nat Genet* **25**, 25–29.

[7] Kononen J, Bubendorf L, Kallioniemi A, Barlund M, Schraml P, Leighton S, Torhorst J, Mihatsch MJ, Sauter G, and Kallioniemi OP (1998). Tissue microarrays for high-throughput molecular profiling of tumor specimens. *Nat Med* **4**, 844–847.

[8] Rand V, Huang J, Stockwell T, Ferriera S, Buzko O, Levy S, Busgam D, Li K, Edwards JB, Eberhard C, et al. (2005). Sequence survey of receptor tyrosine kinases reveals mutations in glioblastomas. *Proc Natl Acad Sci USA* **102**, 14344–14349.

[9] Vajkoczy P, Knyazev P, Kunkel A, Capelle HH, Behrndt S, von Tengg-Kobligk H, Kiessling F, Eichelsbacher U, Essig M, Read TA, et al. (2006). Dominant-negative inhibition of the Axl receptor tyrosine kinase suppresses brain tumor cell growth and invasion and prolongs survival. *Proc Natl Acad Sci USA* **103**, 5799–5804.

[10] Lu C, Shahzad MM, Wang H, Landen CN, Kim SW, Allen J, Nick AM, Jennings N, Kinch MS, Bar-Eli M, et al. (2008). EphA2 overexpression promotes ovarian cancer growth. *Cancer Biol Ther* **7**, 1098–1103.

[11] Kiyokawa E, Takai S, Tanaka M, Iwase T, Suzuki M, Xiang YY, Naito Y, Yamada K, Sugimura H, and Kino I (1994). Overexpression of ERK, an EPH family receptor protein tyrosine kinase, in various human tumors. *Cancer Res* **54**, 3645–3650.

[12] Herath NI, Spanevello MD, Sabesan S, Newton T, Cummings M, Duffy S, Lincoln D, Boyle G, Parson PG, and Boyd AW (2006). Over-expression of Eph and ephrin genes in advanced ovarian cancer: ephrin gene expression correlates with shortened survival. *BMC Cancer* **6**, 144.

[13] Gilmour LM, Macleod KG, McCaig A, Gullick WJ, Smyth JF, and Langdon SP (2001). Expression of erbB-4/HER-4 growth factor receptor isoforms in ovarian cancer. *Cancer Res* **61**, 2169–2176.

[14] Srinivasan R, Gillett CE, Barnes DM, and Gullick WJ (2000). Nuclear expression of the c-erbB-4/HER-4 growth factor receptor in invasive breast cancers. *Cancer Res* **60**, 1483–1487.

[15] Witton CJ, Going JJ, Cooke TG, and Bartlett JM (2003). Expression of the HER1-4 family of receptor tyrosine kinases in breast cancer. *J Pathol* **200**, 290–297.

[16] Sartor CI, Zhou H, Kozlowska E, Guttridge K, Kawata E, Caskey L, Harrelson J, Hynes N, Ethier S, Calvo B, et al. (2001). HER4 mediates ligand-dependent antiproliferative and differentiation responses in human breast cancer cells. *Mol Cell* **21**, 4265–4275.

[17] Vidal GA, Anjali Naresh A, Marrero L, and Jones FE (2005). Presenilin-dependent γ-secretase processing regulates multiple ERBB4/HER4 activities. *JBC* **280**, 19777–19783.

[18] Soung YH, Lee JW, Kim SY, Wang YP, Jo KH, Moon SW, Park WS, Nam SW, Lee JY, Yoo NJ, et al. (2006). Somatic mutations of the ERBB4 kinase domain in human cancers. *Int J Cancer* **118**, 1426–1429.

[19] Rhodes DR, Yu J, Shanker K, Deshpande N, Varambally R, Ghosh D, Barrette T, Pandey A, and Chinnaiyan AM (2004). ONCOMINE: a cancer microarray database and integrated data-mining platform. *Neoplasia* **6**, 1–6.

[20] Hendrix ND, Wu R, Kuick R, Schwartz DR, Fearon ER, and Cho KR (2006). Fibroblast growth factor 9 has oncogenic activity and is a downstream target of Wnt signaling in ovarian endometrioid adenocarcinomas. *Cancer Res* **66**, 1354–1362.

[21] Bild AH, Yao G, Chang JT, Wang Q, Potti A, Chasse D, Joshi MB, Harpole D, Lancaster JM, Berchuck A, et al. (2006). Oncogenic pathway signatures in human cancers as a guide to targeted therapies. *Nature* **439**, 353–357.

[22] Schwartz DR, Kardia SL, Shedden KA, Kuick R, Michailidis G, Taylor JM, Misek DE, Wu R, Zhai Y, Darrah DM, et al. (2002). Gene expression in ovarian cancer reflects both morphology and biological behavior, distinguishing clear cell from other poor-prognosis ovarian carcinomas. *Cancer Res* **62**, 4722–4729.

[23] Welsh JB, Zarrinkar PP, Sapinoso LM, Kern SG, Behling CA, Monk BJ, Lockhart DJ, Burger RA, and Hampton GM (2001). Analysis of gene expression profiles in normal and neoplastic ovarian tissue samples identifies candidate molecular markers of epithelial ovarian cancer. *Proc Natl Acad Sci USA* **98**, 1176–1181.

[24] Lancaster JM, Dressman HK, Whitaker RS, Havrilesky L, Gray J, Marks JR, Nevins JR, and Berchuck A (2004). Gene expression patterns that characterize advanced stage serous ovarian cancers. *J Soc Gynecol Investig* **11**, 51–59.

[25] Gilks CB, Vanderhyden BC, Zhu S, van de Rijn M, and Longacre TA (2005). Distinction between serous tumors of low malignant potential and serous carcinomas based on global mRNA expression profiling. *Gynecol Oncol* **96**, 684–694.

Table W1. List of 69 Ovarian Cell Surface Kinase Genes (203 Probes).

	ProbeSet_id	Gene Name	Gene Symbol	Ref Seq	Kinase	Normal Ovary*	
						ESTS	SAGE
1	203935_at	Activin A receptor, type I	*ACVR1*	NM_001105	STE	21.7	0
2	205209_at, 205209_at, 208218_s_at, 208219_at, 208222_at, 208223_s_at, 213198_at	Activin A receptor, type IB	*ACVR1B*	NM_004302	STE	21.7	2.1
3	205327_s_at, 228416_at	Activin A receptor, type IIA	*ACVR2*	NM_001616	STE	0	0
4	220028_at, 236126_at, 1559548_at	Activin A receptor, type IIB	*ACVR2B*	NM_001106	STE	0	0
5	1552519_at	Activin A receptor, type IC	*ACVR1C*	NM_145259	STE	0	0
6	236126_at	Activin A receptor type II-like 1	*ACVRL1*	NM_000020	STE	0	0
7	208211_s_at, 208212_s_at	Anaplastic lymphoma kinase (Ki-1)	*ALK*	NM_004304	TK	0	0
8	206892_at	Anti-Mullerian hormone receptor, type II	*AMHR2*	NM_020547	STE	0	0
9	202686_s_at	AXL receptor tyrosine kinase	*AXL*	NM_001699	TK	21.7	8.4
10	204832_s_at, 213578_at	Bone morphogenetic protein receptor, type IA	*BMPR1A*	NM_004329	STE	0	2.1
11	210523_at	Bone morphogenetic protein receptor, type IB	*BMPR1B*	NM_001203	STE	0	0
12	209920_at,210214_s_at, 225144_at, 231873_at, 238516_at	Bone morphogenetic protein receptor, type II (serine/threonine kinase)	*BMPR2*	NM_001204	TKL	21.7	10.5
13	203104_at	Colony stimulating factor 1 receptor, formerly McDonough feline sarcoma viral (v-fms) oncogene homolog	*CSF1R*	NM_005211	TK	21.7	0
14	207169_x_at, 208779_x_at, 210749_x_at	Discoidin domain receptor family, member 1	*DDR1*	NM_001954	TK	21.7	10.5
15	205168_at, 225442_at, 227561_at, 235631_at	Discoidin domain receptor family, member 2	*DDR2*	NM_006182	TK	0	10.5
16	1565483_at, 1565484_x_at 201983_s_at, 201984_s_at 210984_x_at, 211550_at 211551_at, 211607_x_at	Epidermal growth factor receptor (erythroblastic leukemia viral (v-erb-b) oncogene homolog, avian)	*EGFR*	NM_005228	TK	21.7	0
17	205977_s_at, 215804_at	EPH receptor A1	*EPHA1*	NM_005232	TK	0	0
18	203499_at	EPH receptor A2	*EPHA2*	NM_004431	TK	0	16.8
19	206070_s_at, 206071_s_at, 211164_at	EPH receptor A3	*EPHA3*	NM_182644	TK	0	0
20	206114_at, 227449_at, 228948_at, 229374_at	EPH receptor A4	*EPHA4*	NM_004438	TK	0	0
21	215664_s_at, 216837_at, 237939_at	EPH receptor A5	*EPHA5*	NM_004439	TK	0	0
22	1561396_at, 233184_at	EPH receptor A6	*EPHA6*	NM_173655	TK	0	0
23	1554629_at, 206852_at, 238533_at	EPH receptor A7	*EPHA7*	NM_004440	TK	0	0
24	1554069_at, 231796_at	EPH receptor A8	*EPHA8*	NM_020526	TK	0	0
25	1553371_at, 236073_at, 243717_at	EPH receptor A10	*EPHA10*	NM_173641	TK	0	0
26	210753_s_at, 211898_s_at, 230425_at	EPH receptor B1	*EPHB1*	NM_004441	TK	0	0
27	209588_at, 209589_s_at, 210651_s_at, 211165_x_at	EPH receptor B2	*EPHB2*	NM_004442	TK	0	4.2
28	1438_at, 204600_at	EPH receptor B3	*EPHB3*	NM_004443	TK	0	0
29	202894_at, 216680_s_at	EPH receptor B4	*EPHB4*	NM_004444	TK	43	2.1
30	204718_at	EPH receptor B6	*EPHB6*	NM_004445	TK	0	0
31	210930_s_at, 216836_s_at, 234354_x_at	V-erb-b2 erythroblastic leukemia viral oncogene homolog 2, neuro/glioblastoma derived oncogene homolog (avian)	*ERBB2*	NM_004448	TK	0	2.1
32	1563252_at, 1563253_s_at, 202454_s_at, 215638_at, 226213_at	V-erb-b2 erythroblastic leukemia viral oncogene homolog 3 (avian)	*ERBB3*	NM_001982	TK	0	27
33	206794_at, 214053_at, 233494_at, 233498_at	V-erb-a erythroblastic leukemia viral oncogene homolog 4 (avian)	*ERBB4*	NM_005235	TK	0	0
34	207822_at, 207937_x_at, 210973_s_at, 211535_s_at, 215404_x_at, 222164_at, 226705_at	Fibroblast growth factor receptor 1 (fms-related tyrosine kinase 2, Pfeiffer syndrome)	*FGFR1*	NM_015850	TK	43	4.2
35	1560859_at, 203638_s_at, 203639_s_at, 208225_at, 208228_s_at, 208229_at, 208234_x_at, 211398_at, 211399_at, 211400_at, 211401_s_at, 240913_at	Fibroblast growth factor receptor 2 (bacteria-expressed kinase, keratinocyte growth factor receptor, craniofacial dysostosis 1, Crouzon syndrome, Pfeiffer syndrome, Jackson-Weiss syndrome)	*FGFR2*	NM_000141	TK	0	10.5
36	204379_s_at, 204380_s_at	Fibroblast growth factor receptor 3 (achondroplasia, thanatophoric dwarfism)	*FGFR3*	NM_000142	TK	0	6.3
37	1554961_at, 1554962_a_at, 204579_at, 211237_s_at	Fibroblast growth factor receptor 4	*FGFR4*	NM_002011	TK	0	0
38	204406_at, 210287_s_at, 222033_s_at, 232809_s_at	Fms-related tyrosine kinase 1 (vascular endothelial growth factor/ vascular permeability factor receptor)	*FLT1*	NM_002019	TK	21.7	0
39	206674_at	Fms-related tyrosine kinase 3	*FLT3*	NM_004119	TK	0	0
40	210316_at, 229902_at, 234379_at	Fms-related tyrosine kinase 4	*FLT4*	NM_182925	TK	21.7	0
41	207851_s_at, 213792_s_at, 226212_s_at, 226216_at, 226450_at	Insulin receptor	*INSR*	NM_000208	TK	65	0
42	203627_at, 203628_at, 208441_at, 225330_at, 243358_at	Insulin-like growth factor 1 receptor	*IGF1R*	NM_000875	TK	65	0
43	215776_at	Insulin receptor-related receptor	*INSRR*	NM_014215	TK	0	0
44	203934_at	Kinase insert domain receptor (a type III receptor tyrosine kinase)	*KDR*	NM_002253	TK	0	2.1
45	205051_s_at	KIT v-kit Hardy-Zuckerman 4 feline sarcoma viral	*KIT*	NM_000222	TK	0	0
46	206223_at, 235307_at	Lemur tyrosine kinase 2	*LMTK2*	NM_014916	TK	0	0
47	1557103_a_at	Lemur tyrosine kinase 3	*LMTK3*	XM_055866	TK	0	0
48	207106_s_at, 217184_s_at	Leukocyte tyrosine kinase	*LTK*	NM_002344	TK	0	0

Table W1. (*continued*)

	ProbeSet_id	Gene Name	Gene Symbol	Ref Seq	Kinase	Normal Ovary*	
						ESTS	SAGE
49	N/A	Similar to bone morphogenetic protein receptor, type IA precursor; activin A receptor, type II-like kinase 3	*LOC283155*	XM_208545	STE	0	0
50	206028_s_at, 211912_at, 211913_s_at, 233079_at	C-mer proto-oncogene tyrosine kinase	*MERTK*	NM_006343	TK	0	0
51	205455_at	Macrophage stimulating 1 receptor (c-met-related tyrosine kinase)	*MST1R*	NM_002447	TK	0	0
52	203510_at, 211599_x_at, 213807_x_at, 213816_s_at	Met proto-oncogene (hepatocyte growth factor receptor)	*MET*	NM_000245	TK	0	0
53	207632_at, 207633_s_at, 241122_s_at,	Muscle, skeletal, receptor tyrosine kinase	*MUSK*	NM_005592	TK	21.7	0
54	208605_s_at	Neurotrophic tyrosine kinase, receptor, type 1	*NTRK1*	NM_002529	TK	0	2.1
55	207152_at, 214680_at, 221795_at, 221796_at, 229463_at, 236095_at	Neurotrophic tyrosine kinase, receptor, type 2	*NTRK2*	NM_006180	TK	0	2.1
56	1557795_s_at, 206462_s_at, 215025_at, 215115_x_at, 217033_x_at, 217377_x_at, 228849_at	Neurotrophic tyrosine kinase, receptor, type 3	*NTRK3*	NM_002530	TK	21.7	0
57	1554828_at, 203131_at, 211533_at, 215305_at	Platelet-derived growth factor receptor, alpha polypeptide	*PDGFRA*	NM_006206	TK	0	16.8
58	202273_at	Platelet-derived growth factor receptor, beta polypeptide	*PDGFRB*	NM_002609	TK	108.5	2.1
59	207011_s_at, 1555324_at	PTK7 protein tyrosine kinase 7	*PTK7*	NM_152883	TK	43	40
60	205879_x_at, 211421_s_at, 215771_x_at	Ret proto-oncogene (multiple endocrine neoplasia and medullary thyroid carcinoma 1, Hirschsprung disease)	*RET*	NM_020630	TK	0	0
61	205805_s_at, 211057_at	Receptor tyrosine kinase-like orphan receptor 1	*ROR1*	NM_005012	TK	0	0
62	205578_at	Receptor tyrosine kinase-like orphan receptor 2	*ROR2*	NM_004560	TK	0	0
63	207569_at	v-ros UR2 sarcoma virus oncogene homolog 1 (avian)	*ROS1*	NM_002944	TK	0	0
64	202853_s_at, 214172_x_at, 216976_s_at	RYK receptor-like tyrosine kinase	*RYK*	NM_002958	TK	65	2.1
65	206702_at, 217711_at	TEK tyrosine kinase, endothelial (venous malformations, multiple cutaneous and mucosal)	*TEK*	NM_000459	TK	0	0
66	206943_at, 224793_s_at, 236561_at	Transforming growth factor, beta receptor I (activin A receptor type II-like kinase, 53kDa)	*TGFBR1*	NM_004612	TKL	0	2.1
67	207334_s_at, 208944_at	Transforming growth factor, beta receptor II (70/80kDa)	*TGFBR2*	NM_003242	TKL	0	6.3
68	1560657_at, 204468_s_a	Tyrosine kinase with immunoglobulin and epidermal growth factor homology domains	*TIE1*	NM_005424	TK	0	18.9
69	211431_s_at, 211432_s_at	TYRO3 protein tyrosine kinase	*TYRO3*	NM_006293	TK	21.7	0

*EST and SAGE counts expressed as normalized values per 200,000 sequences.

Table W2. Oligonucleotide Primers Used in the Semiquantitative RT-PCR Analysis.

Oligonucleotide Sequence	Orientation with Respect to the Transcript	Base Alignment in the Gene	Gene	Exon/Intron Boundary
CAGTGTGACAGTGAGCGACC	S	1343	*EphA2*	Exon 5
cgcaTTGGAGTCTCCCTTCTTGc	AS	1557	*EphA2*	Exon 6, 7
CAGTGGAAGTTGCTGCGAATG	S	2812	*EphA5*	Exon 16
ggcccatcttgattgcctctagcca	AS	2990	*EphA5*	Exon 17
TGCGCTTCACTGTGAGAGAC	S	266	*EphB1*	Exon 10
GAAAGAAGAGACATACAGGCTCC	AS	563	*EphB1*	Exon 11, 12
GACCCTGGTACTTGTGAAGAGCC	S	266	*PTK7*	N/A
CATAGGGCCACCTTCTGCTTGGT	AS	563	*PTK7*	N/A
AATCAAGTACCGCCGCTTG	S	2823	*INSRR*	Exon 13
gcGGTTCTGTTTCTCTTCTTGCcG	AS	3083	*INSRR*	Exon 15, 16
cggaaAGGGCTAAACGGCAATTCcG	S	3530	*ALK*	Exon 15
GATGCCCAGTGGACTGATGAAG	AS	3778	*ALK*	Exon 17
cagctaggcttacagcattgcgga	S	1515	*TGFBR1*	Exon 9
atgatctccagcacagcagag	AS	1912	*TGFBR1*	Exon 11, 12

Table W3. Oncomine Database Analysis of the Expression of Cell Surface Kinases in Ovarian Cancer in 13 Ovarian Cancer Studies.

Gene	Study	Analysis	Observation (No. Patients)	*P*
ALK	Hendrix_	Stage	Upregulated in stage I (35) *vs* IV (9)	2.1E-5
	Lu	Histology	Upregulated in clear cell (7), Endometrioid (9), serous (20) *vs* mucinous (9)	1.2E-4
	Hendrix	Grade	Downregulated in grade 1 (19) *vs* grade 3 (33)	.005
	Lu	Survival	Upregulated in alive (7) *vs* dead (10)	.014
EPHA5	Lu	Histology	Upregulated in clear cell (7), Endometrioid (9), serous (20) *vs* mucinous (9)	8.3E-5
	Gilks_	Grade	Upregulated in low malignant potential (10) *vs* grade 3	.003
	Bild	Stage	Upregulated in IV (21) *vs* III (111)	.04
EPHB1	Gilks_	Grade	Upregulated in low malignant potential (10) *vs* grade 3	.009
	Hendrix	Stage	Upregulated in stage I (35) *vs* IV (9)	.018
	Hendrix	Grade	Downregulated in grade 1 (19) *vs* 3 (33)	.037
ERBB4	Lu	Histology	Upregulated in Clear Cell (7), Endometrioid (9), Serous (20) *vs* Mucinous (9)	5.4E-7
	Hendrix	Tumor type	Upregulated in serous (41) *vs* normal ovary	3.4E-17
	Hendrix	Tumor type	Upregulated in endometrioid (37) *vs* normal ovary	1.2E-11
	Lu	5 years survival	Upregulated in alive (7) vs dead (10)	.023
INSRR	Hendrix	Histology	Upregulated in clear cell (8) *vs* normal ovary (4)	.003
PTK7	Lu	Histology	Upregulated in clear cell (7), endometrioid (9), serous (20) *vs* mucinous (9)	.011
	Schwartz	Histology	Upregulated in clear cell (8), endometrioid (33), mixed histology (9), serous (53) *vs* mucinous (10)	.024
TGFBR1	Gilks	Stage	Upregulated in grade IV (6) *vs* I (1) upregulated in endometriod ovarian carcinoma (9) *vs* clear cell	.012
	Lu	Histology	Ovarian carcinoma (8), mucinous ovarian carcinoma (9), serous ovarian carcinoma (19)	.036
AXL	Lancaster	Histology	Upregulated in normal ovary (3) *vs* ovarian adenocarcinoma (31)	3.2E-13
	Hendrix	Histology	Upregulated in normal ovary (3) *vs* ovarian endometrioid adenocarcinoma (37)	1.3E-5
EPHA2	Lancaster	Histology	Upregulated in normal ovary (3) *vs* ovarian adenocarcinoma (31)	5.8E-6
	Hendrix	Histology	Upregulated in ovarian endometrioid adenocarcinoma *vs* (37) *vs* normal ovary (4)	1.4E-4
	Gilks	Stage	Upregulated in grade I (6) *vs* IV (4)	9.8E-4
PDGFRA	Hendrix	Histology	Upregulated in normal ovary (4) *vs* ovarian serous adenocarcinoma (41)	4.2E-18
	Hendrix	Histology	Upregulated in normal ovary (4) *vs* ovarian endometrioid adenocarcinoma (37)	1.9E-16
	Welsh	Histology	Downregulated in ovarian adenocarcinoma (28) *vs* normal ovary (8)	7E-11
	Lu	Histology	Downregulated in serous ovarian carcinoma (19) *vs* normal ovarian surface epithelium (5)	4.1E-4